Implementation of a Highly Diffusing 2-D Digital Waveguide Mesh with a Quadratic Residue Diffuser

Kyogu Lee, Julius O. Smith
Center for Computer Research in Music and Acoustics (CCRMA)
Music Department, Stanford University
{kglee, jos}@ccrma.stanford.edu

Abstract

In concert hall acoustics, the reflection characteristics of the ceiling and the walls are important for minimizing the interaural cross correlation. Many design methods have been presented so far in order to design highly diffusing surfaces. This paper presents a two-dimensional digital waveguide mesh having a highly diffusing boundary using quadratic residue sequences, and illustrates its reflection properties. Empirical analyses show that high diffusion occurs at the diffusing boundary, and the scattering characteristics show the energy of an incident plane wave is evenly scattered in a mesh with a diffusing boundary while a specular reflection occurs in a mesh with flat surfaces.

1 Introduction

In an ideal concert hall, the reverberant response should be smooth, dense, and free of overly prominent resonances and reflections. While this is theoretically impossible at all frequencies in a typical concert-hall geometry, the reverberant response can be improved in a variety of ways. In particular, it is desirable that reflected sound waves in the hall *scatter* as uniformly as possible throughout the audience. That is, rather than having *specular* reflections, which are analogous to light reflecting from a mirror, we prefer *diffuse* reflections—more analogous to the scattered light which illuminates the daytime sky.

In the 1970s, Schroeder proposed methods of designing highly diffusing surfaces based on maximum-length sequences and quadratic residue sequences (Schroeder 1975; Schroeder 1979). These so-called *quadratic residue diffusers* (QRD) have been widely applied to the design of recording studios and concert halls. In the 1960s, Schroeder also initiated the topic of *artificial reverberation* (Schroeder and Logan 1961; Schroeder 1970), in which digital filter structures (particularly allpass filters) were used to simulate "colorless" reverberation. The use of allpass filters guaranteed an equal reverberant response at all frequencies, while a QRD guarantees an equal reflection strength at some number of frequencies and reflection angles.

In 1993, Van Duyne and Smith introduced an efficient way of modeling wave propagation in a membrane using a 2-D digital waveguide mesh, and showed that it coincided with a standard finite difference approximation scheme for the 2-D wave equation (Van Duyne and Smith 1993b). The mesh has also been applied to the problem of artificial reverberation (Smith 1985; Savioja, Backman, Järvinen, and Takala 1995; Huang, Serafin, and Smith 2000; Laird, Masri, and Canagarajah 1999; Murphy and Howard 2000; Murphy, Newton, and Howard 2001).

In this paper, the 2-D digital waveguide mesh is extended to include a diffusing boundary based on a Schroeder quadratic residue diffuser. First we review quadratic residue diffusers and the 2-D digital waveguide mesh, followed by implementation details and simulation results.

2 The Quadratic Residue Diffuser

Schroeder presented methods of designing concert hall ceilings that could avoid direct reflections into the audience. In 1975, he provided a way of designing highly diffusing surfaces based on binary maximum-length sequences, and showed that these periodic sequences have the property that their harmonic amplitudes are all equal (Schroeder 1975). He later extended his method and proposed surface structures that give excellent sound diffusion over larger bandwidths (Schroeder 1979). This is based on quadratic residue sequences of elementary number theory, investigated by A. M. Legendre and C. F. Gauss. These sequences are defined by

$$s_n = n^2 \quad (\bmod N), \tag{1}$$

i.e., n^2 is taken as the least nonnegative remainder modulo N, and N is an odd prime number. For $N = 17$, the quadratic residue sequence reads as follows (starting with $n = 0$):

$$s_n = 0, 1, 4, 9, 16, 8, 2, 15, 13, 13, 15, 2, 8, 16, 9, 4, 1; 0, 1, \cdots$$

These sequences have a few properties:

1. they are symmetric [around $n \equiv 0$ and $n \equiv (N-1)/2$];
2. they are periodic with period N;
3. surprisingly, the discrete Fourier transform R_m of the exponentiated sequence

$$r_n = e^{\pm j2\pi s_n/N} \tag{2}$$

has constant magnitude

$$|R_m| = \left| \frac{1}{N} \sum_{n=1}^{N} r_n e^{-j2\pi nm} \right|^2 = \frac{1}{N}. \tag{3}$$

The quadratic residue diffuser, or Schroeder diffuser, is implemented by having periodic wells of different depths proportional to s_n with period N over the surface. Figure 1 shows a cross section through the diffusing surface based on the quadratic residue sequence with $N = 17$.

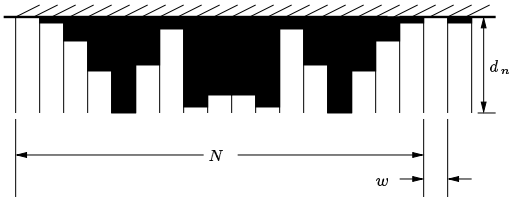

Figure 1: Cross section through a highly diffusing surface based on quadratic residue sequence when $N = 17$. The thin vertical lines represent rigid separators between individual wells.

The width of each well w is determined by the design wavelength $\lambda_0 (\gg w)$, and the depths of the well d_n are defined as

$$d_n = \frac{\lambda_0}{2N} s_n, \tag{4}$$

where s_n is the quadratic residue sequence with period N.

Strube did empirical and numerical analyses on scattering characteristics of Schroeder's diffuser (Strube 1980a; Strube 1980b), and design techniques of concert halls were provided by Ando using Schroeder's diffuser (Ando 1985).

3 The 2-D Digital Waveguide Mesh

Digital waveguide techniques have been used to develop efficient physical models of musical instruments since the early 1990s (Smith 1987; Smith III 2003; Van Duyne and Smith 1993a; Van Duyne and Smith 1993b). The digital waveguide model can be used to reduce the computational cost of physical models based on numerical integration of the wave equation by three orders of magnitude by simulating the traveling waves with digital delay lines.

The one-dimensional digital waveguide can be extended into a two-dimensional digital waveguide mesh (Van Duyne and Smith 1993a; Van Duyne and Smith 1993b). The structure of the 2-D digital waveguide mesh can be viewed as a layer of parallel vertical waveguides superimposed on a layer of parallel horizontal waveguides intersecting each other at 4-port scattering junctions as shown in Figure 2.

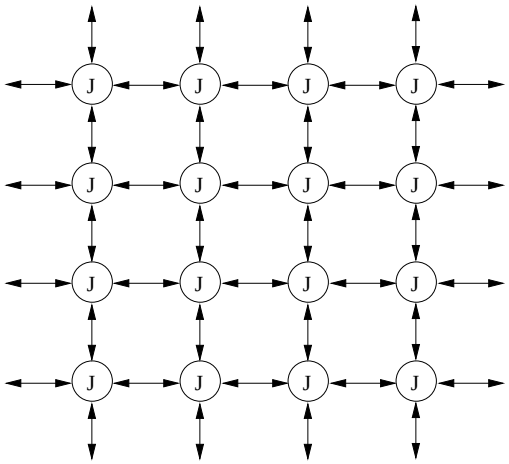

Figure 2: The 2-D digital waveguide mesh.

In a lossless case, the scattering junction has two physical constraints: 1) the velocities of all the strings at the junction must be equal, i.e.,

$$v_1 = v_2 = \cdots = v_N, \tag{5}$$

and 2) the forces exerted by all the strings must sum to zero, i.e.,

$$f_1 + f_2 + \cdots + f_N = 0, \tag{6}$$

where N is the number of strings.

Combining the two series junction constraints with the wave impedance relations between force and velocity wave variables defined as $f^+ = Rv^+$ and $f^- = -Rv^-$, and with the wave variable definitions, $v_i = v_i^+ + v_i^-$, and $f_i = f_i^+ + f_i^-$, we can derive the lossless scattering equations for the junctions in which four strings intersect,

$$v_J = \frac{2\sum_{i=1}^{4} R_i v_i^+}{\sum_{i=1}^{4} R_i}, \tag{7}$$

$$v_i^- = v_J - v_i^+, \tag{8}$$

where v_J represents the junction velocity, and the v_i^+'s and the v_i^-'s are the incoming and the outgoing waves at the junction, respectively. Assuming an isotropic membrane, where

$R_1 = R_2 = R_3 = R_4$, Equation 7 further simplifies to

$$v_J = \frac{v_1^+ + v_2^+ + v_3^+ + v_4^+}{2}. \quad (9)$$

4 Implementation and Results

4.1 Implementation of Boundary with the Wells

The 2-D digital waveguide mesh can be implemented by having bi-directional unit delay lines between adjacent junctions as shown in Figure 3.

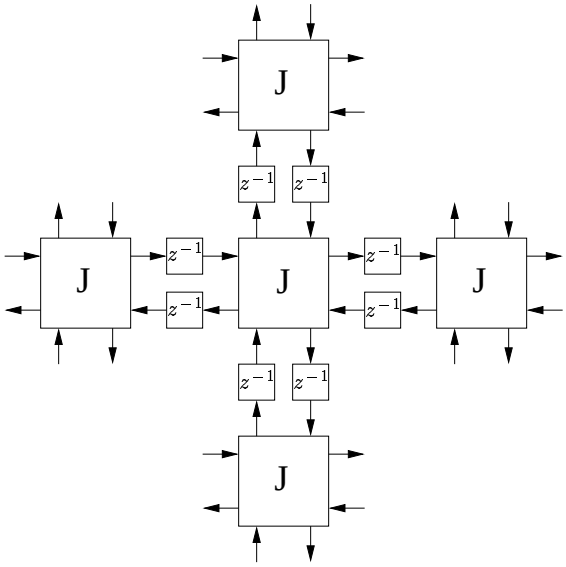

Figure 3: The 2-D digital waveguide mesh with bi-directional unit delay lines.

In order to simulate the boundary with the wells of different depths in a 2-D digital waveguide mesh, we need to convert the depths of the wells in Equation 4 to the number of junctions. Since the travel time of the wave in the nth well is given by

$$t_n = \frac{d_n}{c}, \quad (10)$$

where d_n is the depth of the nth well, and c is the speed of the sound, we can calculate the travel time in samples for the traveling wave by multiplying Equation 10 by the sampling rate, i.e.,

$$n_n = t_n f_s = \frac{d_n}{c} f_s, \quad (11)$$

where n_n is the travel time in samples in the nth well and f_s is the sampling rate. Substituting d_n with that in Equation 4 yields

$$n_n = \frac{\lambda_0}{2N} \frac{f_s}{c} s_n, \quad (12)$$

where s_n is a quadratic residue sequence with period N.

Since the wells are rigidly separated from each other in Schroeder's diffuser, we need to take this into account when implementing it in a 2-D digital waveguide mesh. This can be accomplished by disconnecting all the horizontal strings between adjacent junctions in the wells as shown in Figure 4. The disconnection of the strings between junctions means the junctions in the wells are no more considered 4-port junctions, and this changes the scattering coefficients. In fact, the junctions in the wells are now pure digital delay lines without any scattering, having reflections only at the end of the wells. The junctions are terminated at the boundaries with a reflection coefficient of 0.999.

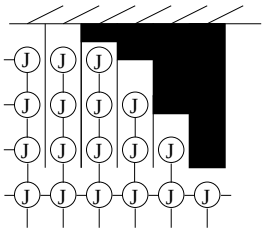

Figure 4: The 2-D digital waveguide mesh in the vicinity of diffusing boundary. Note there are no horizontal connections between junctions in the wells.

The design wavelength λ_0 used in our simulation is 25 cm, and each well is one sample wide, which gives the well width of $w = cT = c/f_s \approx 1.56\,cm$ ($\ll \lambda_0$). Therefore, the $\lambda_0 \gg w$ requirement in Schroeder's diffuser has been satisfied.

4.2 Empirical Analysis

We have modified the algorithm for the rectilinear mesh in such a way that Schroeder's diffuser is implemented on one of its boundaries, and compared them by visualizing the meshes at different time frames. Figure 5 shows wave propagation on the rectilinear mesh with rigid, flat boundaries which yield specular reflections when given an initial excitation at the center.

The figure shows that specular reflections occur at the boundaries. We can clearly see the symmetry in the wave propagation pattern, and the energy is concentrated at some regions in the mesh after some time has passed. On the other hand, the mesh with one of its boundaries being replaced with Schroeder's diffuser reveals very different reflection characteristics as shown in Figure 6. The wave propagates in the same pattern at the beginning as in the plain mesh, but it starts to diffuse in the third plot as it approaches a boundary with Schroeder's diffuser. This diffusion from the the uneven boundary disturbs the symmetric wave propagation pattern

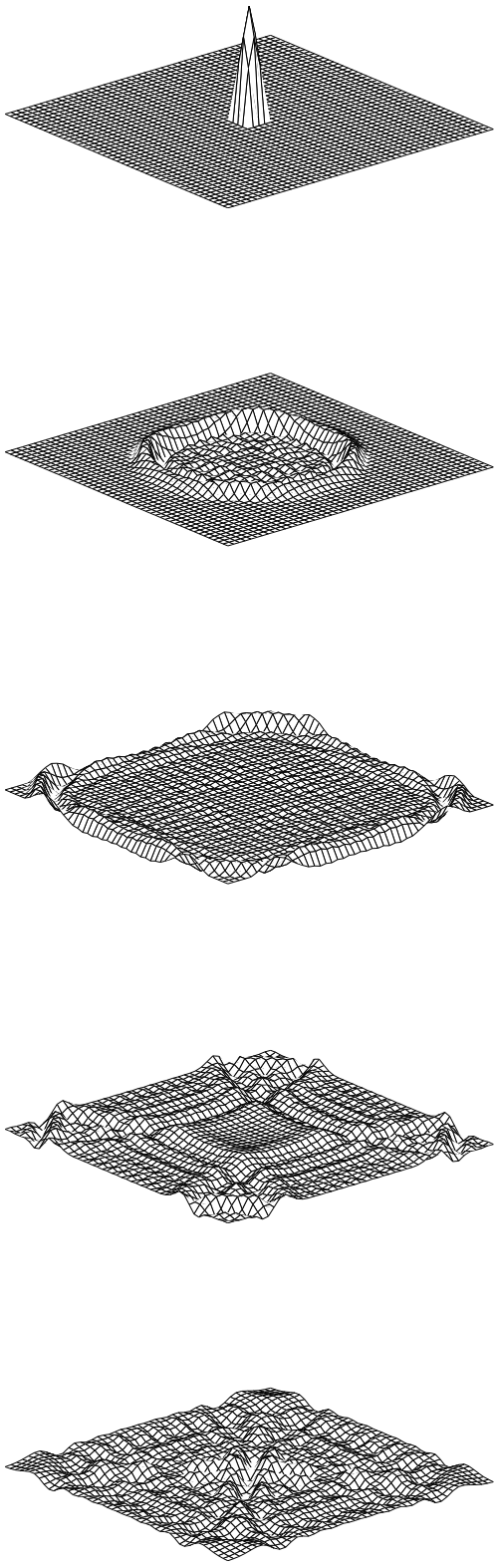

Figure 5: Wave propagation on the mesh with flat surfaces at time frames $n = 1, 20, 40, 60, 100$, respectively.

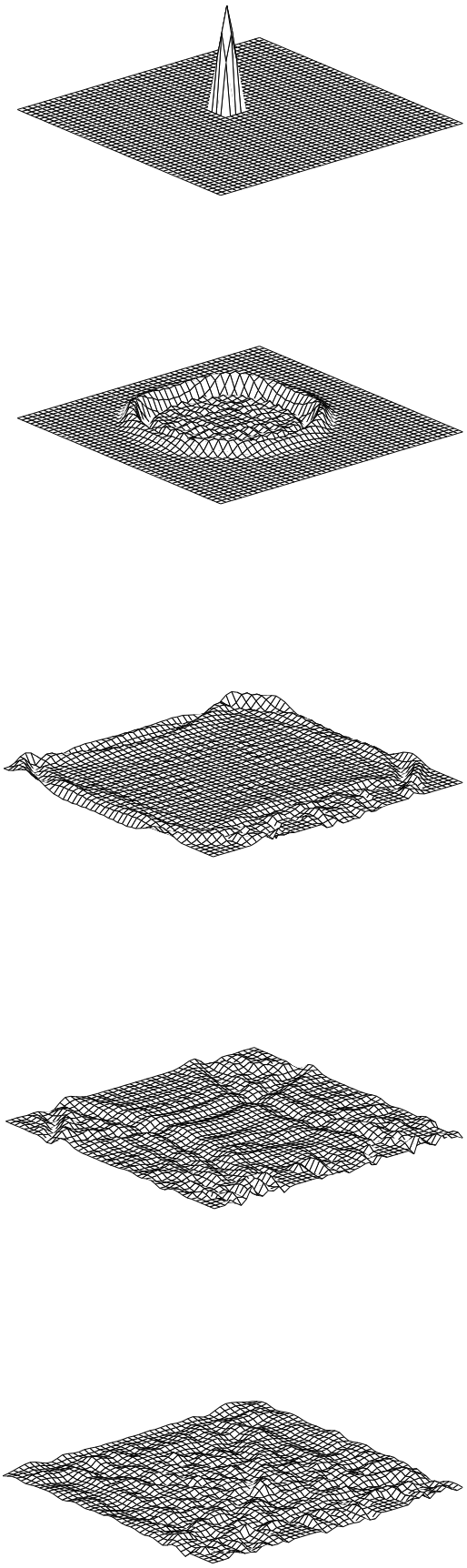

Figure 6: Wave propagation on the mesh with Schroeder's diffuser when N = 17 (diffusing surface at bottom-right side).

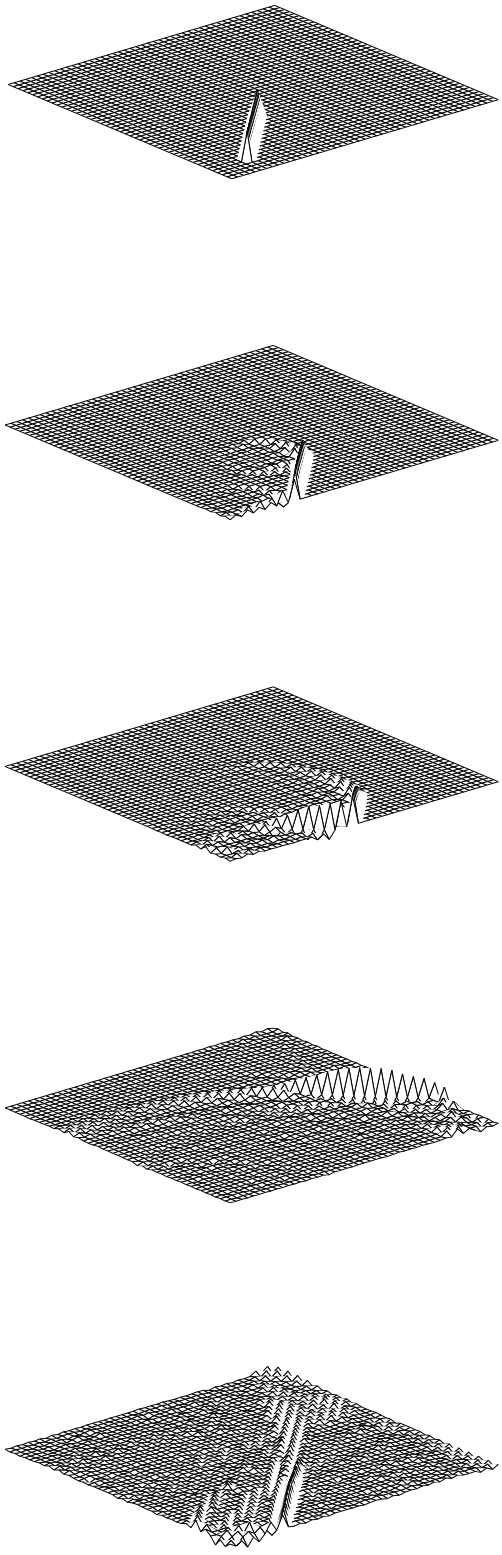

Figure 7: Plane wave propagation on the mesh with flat surfaces at time frames $n = 1, 10, 20, 60, 200$, respectively.

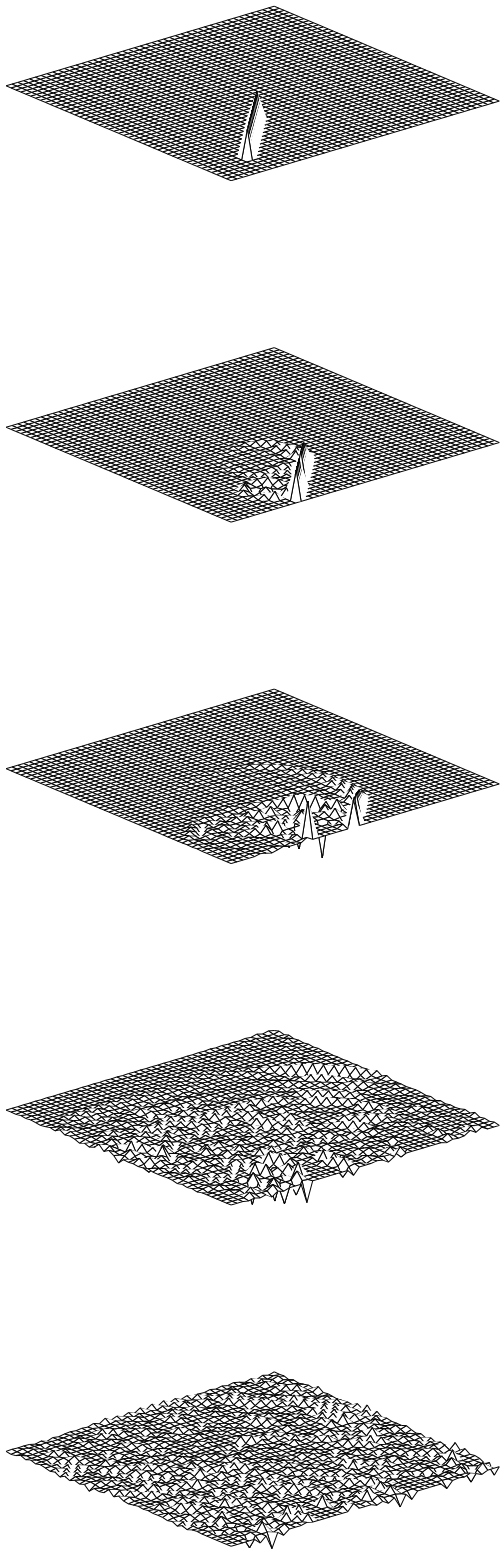

Figure 8: Plane wave propagation on the mesh with Schroeder's diffuser when N = 17 (diffusing surface at bottom-right side).

seen in the plain mesh, and in the last plot, we can see the energy is evenly distributed all over the mesh after a very short period of 4.5 milliseconds.

The comparison between the plain mesh with specular boundaries and the mesh with a diffusing boundary becomes more obvious if we use an incident plane wave as their initial excitation. Even before looking at the animated results, we may expect that the plain mesh with flat surfaces will show a specular reflection pattern; i.e., the plane wave will reflect with equal angles of incidence and reflection as light is reflected in the mirror. Figure 7 shows this specular reflection of the plane wave when the angle of incidence is $\alpha = 45°$. The plane wave is reflected with the same angle as its angle of incidence, and keeps the same specular reflection pattern, resulting in the propagation pattern similar to diamond shape, whereas the wave propagation pattern shown in Figure 8 is totally different. The plane wave is diffused as it reaches the diffusing surface in the second plot, and it starts to propagate in many directions as shown in the next plot. Finally, in the last plot, we can see the sound energy is evenly distributed on the mesh without any visible concentration on specific regions.

We have measured scattering levels at various angles in the vicinity of the boundaries by using a half-plane wave normal to the reflection boundary as an excitation source (i.e., incidence angle of $\alpha = 0°$), and by having multiple reception points along the line parallel to the boundary as shown in Figure 9. The resulting polar responses shown in Figure 10 clearly show that the sound energy is evenly scattered at every angle at the diffusing boundary. On the other hand, in case of the flat surface, most of the energy is centered on the receiver where the reflection angle is $0°$ due to specular reflection.

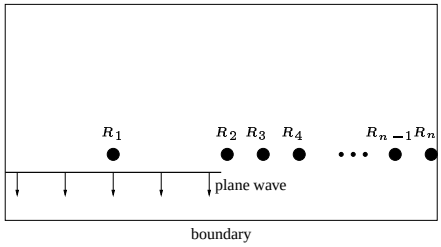

Figure 9: 128x64 rectilinear mesh with a half-plane wave and multiple reception points.

Note that sound examples and Matlab generated movies which clearly visualize wave propagation are available from the WWW URL address: `http://www-ccrma.stanford.edu/~kglee/2dmesh_QRD/`

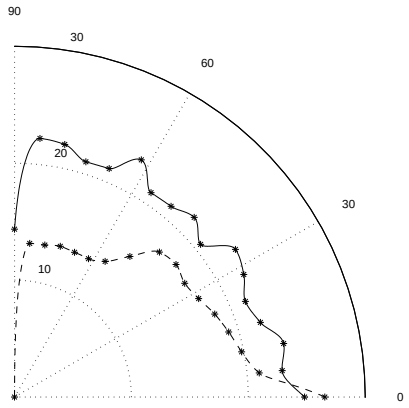

Figure 10: Scattering levels from a Schroeder's diffuser (solid) and a flat surface (dashed).

5 Conclusions

Schroeder's diffusers proved to be very successful, and alternate designs as well as its original design have been applied to concert halls to evenly distribute the sound energy to the audience area (Cox and D'Antonio 2003). In this paper, we have implemented a 2-D digital waveguide mesh with Schroeder's diffuser based on quadratic residue sequences, and have simulated its performance. We have shown that the diffusion occurs at the boundary in a mesh where Schroeder's diffuser is implemented, the sound energy is evenly dispersed everywhere after a while. On the other hand, a plain mesh shows more specular reflections, and the sound energy is more concentrated in some regions in a specific pattern. The computational efficiency of the 2-D digital waveguide mesh is largely preserved, since computations along the boundary of an $N \times N$ mesh are $\mathcal{O}(N)$, while the time-update for the entire mesh is $\mathcal{O}(N^2)$. This highly diffusing 2-D digital waveguide mesh may be extended to implement artificial reverberation, or to model a musical instrument's body.

References

Ando, Y. (1985). *Concert Hall Acoustics*. Springer-Verlag.

Cox, T. J. and P. D'Antonio (2003). Engineering art: the science of concert hall acoustics. *Interdisciplinary Scicence Review 28*(2), 119–129.

Huang, P., S. Serafi n, and J. Smith (2000, Aug.). A waveguide mesh model of high-frequency violin body resonances. In *Proceedings 2000 International Computer Music Conference, Berlin.*

Laird, J., P. Masri, and N. Canagarajah (1999, October). Modelling diffusion at the boundary of a digital waveguide mesh.

In *Proceedings of the International Computer Music Conference*, Beijing, China.

Murphy, D. T. and D. M. Howard (2000, December). 2-D digital waveguide mesh topologies in room acoustics modelling. In *Proceedings of the COST G-6 Conference on Digital Audio Effects (DAFx)*, Verona, Italy, pp. 211–216.

Murphy, D. T., C. J. C. Newton, and D. M. Howard (2001, December). Digital waveguide mesh moelling of room acoustics: surround-sound, boundaries and plugin implementation. In *Proceedings of the COST G-6 Conference on Digital Audio Effects (DAFx)*, Limerick, Ireland.

Savioja, L., J. Backman, A. Järvinen, and T. Takala (1995, June). Waveguide mesh method for low-frequency simulation of room acoustics. *Proceedings 15th International Conference on Acoustics (ICA-95), Trondheim, Norway*, 637–640.

Schroeder, M. R. (1970). Digital simulation of sound transmission in reverberant spaces (part i). *Journal of the Acoustical Society of America 47*(2), 424–431.

Schroeder, M. R. (1975). Diffuse sound reflection by maximum-length sequence. *Journal of the Acoustical Society of America 57*(1), 149–150.

Schroeder, M. R. (1979). Binaural dissimilarity and optimum ceilings for concert halls: More lateral sound diffusion. *Journal of the Acoustical Society of America 65*(4), 958–963.

Schroeder, M. R. and B. F. Logan (1961). Colorless artificial reverberation. *IRE Transactions AU-9*, 209–214.

Smith, J. O. (1985). A new approach to digital reverberation using closed waveguide networks. pp. 47–53. Computer Music Association. also available in (Smith 1987).

Smith, J. O. (1987). Music applications of digital waveguides. Technical Report STAN–M–39, CCRMA, Music Department, Stanford University. a compendium containing four related papers and presentation overheads on digital waveguide reverberation, synthesis, and filtering. CCRMA technical reports can be ordered by calling (650)723-4971 or by sending an email request to info@ccrma.stanford.edu.

Smith III, J. O. (2003). *Digital Waveguide Modeling of Musical Instruments*. `http://www-ccrma.stanford.edu/~jos/waveguide/`.

Strube, H. W. (1980a). Diffraction by a planar, locally reacting, scattering surface. *Journal of the Acoustical Society of America 67*(2), 460–469.

Strube, H. W. (1980b). Scattering of a plane wave by a schroeder diffusor: A mode-matching approach. *Journal of the Acoustical Society of America 67*(2), 453–459.

Van Duyne, S. A. and J. O. Smith (1993a, Oct.). The 2-D digital waveguide mesh. In *Proceedings IEEE Workshop on Applications of Signal Processing to Audio and Acoustics, New Paltz, NY*, New York. IEEE Press.

Van Duyne, S. A. and J. O. Smith (1993b). Physical modeling with the 2-D digital waveguide mesh. In *Proceedings 1993 International Computer Music Conference, Tokyo*, pp. 40–47. Computer Music Association. available online at `http://-www-ccrma.stanford.edu/~jos/pdf/mesh.pdf`.